Biogeosciences, 11, 5675–5686, 2014
www.biogeosciences.net/11/5675/2014/
doi:10.5194/bg-11-5675-2014
© Author(s) 2014. CC Attribution 3.0 License.

Biogeosciences
Open Access

Soil–atmosphere exchange of ammonia in a non-fertilized grassland: measured emission potentials and inferred fluxes

G. R. Wentworth, J. G. Murphy, P. K. Gregoire, C. A. L. Cheyne, A. G. Tevlin, and R. Hems

Department of Chemistry, University of Toronto, 80 St. George Street, M5S 3H6, Toronto, Canada

Correspondence to: J. G. Murphy (jmurphy@chem.utoronto.ca)

Received: 5 March 2014 – Published in Biogeosciences Discuss.: 27 May 2014
Revised: 12 September 2014 – Accepted: 15 September 2014 – Published: 16 October 2014

Abstract. A 50-day field study was carried out in a semi-natural, non-fertilized grassland in south-western Ontario, Canada during the late summer and early autumn of 2012. The purpose was to explore surface–atmosphere exchange processes of ammonia (NH_3) with a focus on bi-directional fluxes between the soil and atmosphere. Measurements of soil pH and ammonium concentration ($[NH_4^+]$) yielded the first direct quantification of soil emission potential ($\Gamma_{soil} = [NH_4^+]/[H^+]$) for this land type, with values ranging from 35 to 1850 (an average of 290). The soil compensation point, the atmospheric NH_3 mixing ratio below which net emission from the soil will occur, exhibited both a seasonal trend and diurnal trend. Higher daytime and August compensation points were attributed to higher soil temperature. Soil–atmosphere fluxes were estimated using NH_3 measurements from the Ambient Ion Monitor Ion Chromatograph (AIM-IC) and a simple resistance model. Vegetative effects were ignored due to the short canopy height and significant Γ_{soil}. Inferred fluxes were, on average, $2.6 \pm 4.5\,ng\,m^{-2}\,s^{-1}$ in August (i.e. net emission) and $-5.8 \pm 3.0\,ng\,m^{-2}\,s^{-1}$ in September (i.e. net deposition). These results are in good agreement with the only other bi-directional exchange study in a semi-natural, non-fertilized grassland. A Lagrangian dispersion model (Hybrid Single-Particle Lagrangian Integrated Trajectory – HYSPLIT) was used to calculate air parcel back-trajectories throughout the campaign and revealed that NH_3 mixing ratios had no directional bias throughout the campaign, unlike the other atmospheric constituents measured. This implies that soil–atmosphere exchange over a non-fertilized grassland can significantly moderate near-surface NH_3 concentrations. In addition, we provide indirect evidence that dew and fog evaporation can cause a morning increase of $[NH_3]_g$. Implications of our findings on current NH_3 bi-directional exchange modelling efforts are also discussed.

1 Introduction

Atmospheric ammonia ($NH_{3(g)}$) is the most abundant alkaline gas and is important for many biogeochemical and atmospheric processes (Seinfeld and Pandis, 2006). It neutralizes acidic aerosol, leading to increased mass loadings of fine atmospheric particulate matter ($PM_{2.5}$), which reduces visibility and can cause adverse health effects (Pope et al., 2002). In addition, deposition of NH_3 and other forms of reactive nitrogen (i.e. NO_x, HNO_3) can lead to eutrophication, soil acidification, and loss of biodiversity in sensitive ecosystems (Krupa, 2003). NH_3 is primarily emitted through agricultural activities (i.e. fertilization, animal waste) with minor contributions from transportation and chemical industries (Reis et al., 2009).

$NH_{3(g)}$ exists in equilibrium with aqueous ammonia ($NH_{3(aq)}$) in surface reservoirs (i.e. apoplastic tissues of plants or soil pore water) that, at least in theory, can be described by the Henry's law constant (K_H). $NH_{3(aq)}$ is also in equilibrium with aqueous-phase ammonium ($NH_{4(aq)}^+$), governed by the acid dissociation constant (K_a) of NH_4^+ and the pH of the solution. The gas-phase concentration above this aqueous phase at thermodynamic equilibrium is known as the compensation point (χ) and can, to a first approximation, be predicted according to

$$\chi = \frac{K_a \cdot [NH_{4(aq)}^+]}{K_H \cdot [H^+]}, \quad (1)$$

where $[H^+]$ is the concentration of the hydronium ion in solution. If the atmospheric mixing ratio of NH_3 over a surface

is below this value, net emission from the surface pool will be expected until the equilibrium NH_3 value (i.e. χ) is reached and vice versa. In order to account for the temperature dependence of the equilibrium constants, the van 't Hoff equation must be applied so Eq. (1) can be updated to

$$\chi = 13587 \cdot \Gamma \cdot e^{\frac{-10396K}{T}} \times 10^9, \quad (2)$$

where T is the temperature of the surface reservoir in K, Γ is the emission potential equal to the ratio between $[NH_4^+]$ and $[H^+]$ in the surface reservoir ($\Gamma = [NH_4^+]/[H^+]$), and χ is given in ppb or nmol mol^{-1} (Nemitz et al., 2001, 2004). A large Γ indicates the surface has a high propensity to emit NH_3 since it is directly proportional to χ. Values for K_H ($10^{-1.76}$ atm M^{-1}) and enthalpy of vaporization (34.18 kJ mol^{-1}) at 25 °C were obtained from Dasgupta and Dong (1986). The K_a and enthalpy of dissociation of NH_4^+ at 25 °C are $10^{-9.25}$ M and 52.21 kJ mol^{-1}, respectively (Bates and Pinching, 1950).

This conceptual model of a compensation point for NH_3 was first suggested by Farquhar et al. (1980). Over the subsequent decades, numerous laboratory and field studies over a wide range of land types have been undertaken to validate and improve this framework. Single-layer exchange models were developed in the 1990s to account for bi-directional exchange with plant stomata and deposition to the cuticle (e.g. Sutton et al., 1993, 1995, 1998). A two-layer model was developed by Nemitz et al. (2001) that also included exchange with the soil. Nemitz et al. (2000) were able to create a multi-layer model that allowed for exchange with different layers within the canopy (i.e. inflorescences, bottom leaves) of oilseed rape. The flux of NH_3 (F_{NH_3}) above a surface reservoir can be calculated from χ with an exchange velocity (ν_{ex}) using the following:

$$F_{NH_3} = \nu_{ex} \cdot (\chi - [NH_{3(g)}]) \quad (3)$$

The ν_{ex} (units of m s^{-1}) can be parameterized by applying resistances in either a series and/or parallel schematic. These resistances represent physical barriers to mass transfer and are analogous to electrical resistances. The number of resistances applied is dependent on how many surface reservoirs are incorporated into the field-scale model. In all cases, aerodynamic (R_a) and quasi-laminar (R_b) resistances must be considered to account for the turbulence between the surface reservoir and $NH_{3(g)}$ measurement height.

Numerous pathways are present for bi-directional exchange over land: via plant stomata, soil pore water, and ground litter. For each compartment there exists a χ which is dependent on the surface properties given in Eqs. (1) and (2). Significant effort has gone into measuring and modelling NH_3 fluxes over a wide variety of land types to provide a more thorough understanding of this framework (Massad et al., 2010; Zhang et al., 2010, and references therein). Canopy-scale resistance models of varying complexity have been developed and successfully employed to mechanistically describe NH_3 fluxes (e.g. Nemitz et al., 2001; Personne et al., 2009; Sutton et al., 1995). A detailed list of these models is available in Flechard et al. (2013).

While extremely useful, these mechanistic canopy-scale models are often too complex to be directly incorporated into regional or global chemical transport models. As a result, recent efforts have focused on simplifying previous models by empirically parameterizing certain components (usually Γ) with either a constant for each land type or a function using parameters (i.e. fertilizer application, regional long-term NH_3 concentration) that are easily assimilated into the regional and global models (Bash et al., 2013; Cooter et al., 2010, 2012; Pleim et al., 2013; Wen et al., 2013; Wichink Kruit et al., 2010, 2012). Incorporating bi-directional NH_3 exchange in these large-scale atmospheric models generally improves model performance. For instance, Bash et al. (2013) reduced the biases and error in both NH_x deposition and aerosol concentration by coupling CMAQ (Community Multiscale Air-Quality) to an agro-ecosystem model and allowing for bi-directional exchange over the continental United States. Wichink Kruit et al. (2012) incorporated bi-directional exchange in the chemical transport model LOTOS-EUROS and found better agreement between measured and modelled NH_3 mixing ratios across Europe, although some domains were still biased low by up to a factor of 2. Large uncertainties still exist for the parameterizations of Γ for both stomata and soil over most land types as a result of sparse measurements. Field measurements of soil and vegetation $[NH_4^+]$ and $[H^+]$, along with atmospheric NH_3 mixing ratios, are required to evaluate the performance of regional air quality models attempting to parameterize bi-directional exchange.

Reviews by Massad et al. (2010) and Zhang et al. (2010) have summarized the studies to date that have explored bi-directional surface–atmosphere NH_3 fluxes over a wide variety of different land types. The majority have focused on biosphere–atmosphere (i.e. stomatal) or canopy–atmosphere (i.e. sum of stomatal, litter, and soil) exchange. In the former, both stomatal and cuticular resistances are incorporated (Massad et al., 2010 and references therein). Indeed, there have been a limited number of studies strictly examining soil–atmosphere bi-directional exchange. One reason is that if a significant canopy (i.e. forest or crops) is present, a significant fraction of soil NH_3 emissions are expected to be recaptured by the canopy before leaving it (Nemitz et al., 2000). For instance, Walker et al. (2013) estimated that $\sim$76 % of soil NH_3 emissions are recaptured by the canopy in a fertilized corn field during peak leaf area index (LAI).

Agricultural fields and fertilized croplands have traditionally been the focus of NH_3 bi-directional exchange studies due to their high propensity to emit NH_3 (Massad et al., 2010; Zhang et al., 2010 and references therein). Semi-natural and non-fertilized ecosystems have been examined less often. Although these areas are much less likely to be large sources

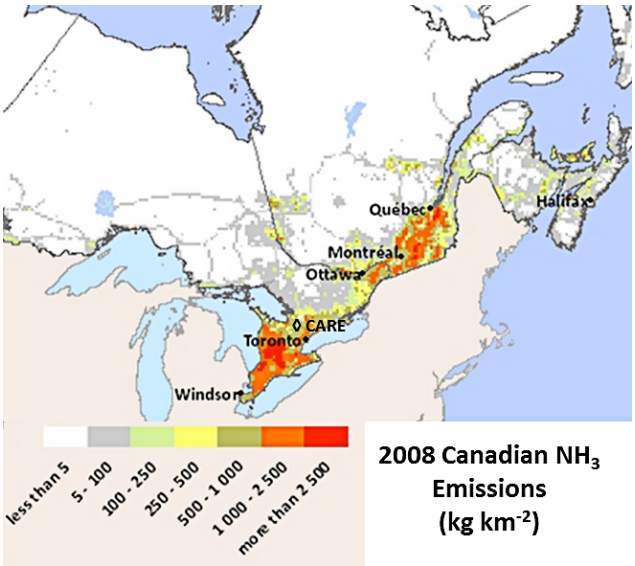

Figure 1. Location of CARE (◊) and major cities in the surrounding area. The map is coloured by annual NH_3 emissions according to the 2008 emission inventory.

of NH_3, they account for a large land fraction and have the potential to impact the quality of atmospheric ammonia predictions from these updated regional-scale models. In particular, there have been fewer studies measuring NH_3 fluxes over grasslands (e.g. Mosquera et al., 2001; Spindler et al., 2001). Several studies (David et al., 2009; Herrmann et al., 2009; Milford et al., 2001; Sutton et al., 2001, 2009) have explored how different grassland management practices (cutting and fertilization) affect NH_3 fluxes; however, all of these studies were performed in fields that had received some degree of fertilization within the last 10 years. To our knowledge, only Wichink Kruit et al. (2007) have investigated NH_3 bi-directional exchange over a non-fertilized grassland. The authors used several denuders and the aerodynamic gradient method to measure fluxes above the canopy and then infer both a canopy χ and Γ.

Motivated by a lack of measurements in non-fertilized grasslands, this present study aims to measure χ and Γ to provide a better constraint on these values since they are directly employed in current air quality models that represent bi-directional exchange. Atmospheric measurements are then used to estimate a soil–atmosphere flux based on a simple resistance model that has been utilized in the past (e.g. Nemitz et al., 2001). Furthermore, we present evidence that bi-directional exchange over a non-fertilized grassland can significantly impact near-surface NH_3 concentrations, and that evaporation of dew can release large quantities of NH_3.

2 Methods and materials

2.1 Field site

Measurements were taken from 12 August to 2 October 2012 at a rural site near Egbert, ON, located approximately 70 km north of Toronto. The long-term sampling site, Centre for Atmospheric Research Experiments (CARE, 44°13′51″ N, 79°46′58″ W, 251 m a.s.l.), is operated by Environment Canada and situated in an agricultural area. Figure 1 shows the location of CARE in relation to major Canadian cities and is coloured according to annual NH_3 emissions from 2008 (NPRI, 2008). Canada's National Pollutant Release Inventory (NPRI) does not include soil or vegetative emissions from non-managed ecosystems. The site is located on a sharp transition with high NH_3 emissions to the south and negligible emissions to the north. Air masses originating from the south are typically polluted since they pass over urban, industrial, and agricultural areas of southern Ontario and the north-eastern United States, whereas cleaner air usually arrives from the north (e.g. Rupakheti et al., 2005). As a result, soil–atmosphere exchange of NH_3 can be examined under a wide range of atmospheric pollution regimes.

The site itself is surrounded by 60 ha of semi-natural, non-fertilized grassland with no overlying canopy. The month of August was relatively dry with cumulative precipitation totalling 8 mm, whereas September had 75 mm of precipitation. The soil sampling area is contained within a radius of 10 m as this is the approximate flux footprint of the air sampling instrumentation explained in Sect. 2.4. Fertilizer has not been applied to the soil in at least 15 years. Grass at the site was cut on 27 June but remained uncut for the duration of the study. Over the course of the study, the grass grew from about 10 cm to a final height of 20 cm. The soil is sandy loam with an organic carbon content of roughly 5 % and a cation exchange capacity (CEC) of 22.7 cmol kg^{-1}. The CEC reflects the soil's ability to retain cations (including NH_4^+) and at this site is an intermediate value relative to other soils.

2.2 Bi-directional exchange framework

For surfaces with minimal vegetation and a high soil emission potential (Γ_{soil}), the exchange between the soil and atmosphere is expected to dominate the bi-directional flux (Personne et al., 2009; Sutton et al., 2009). In these environments, it should be reasonable to estimate v_{ex} by only considering resistances affecting the exchange across the soil–atmosphere interface. As such, v_{ex} in this paper is approximated using Eq. (4), which was derived from Su et al. (2011), who parameterized HONO soil fluxes in a similar fashion. This method is also the same as the two-layer resistance model developed by Nemitz et al. (2001) but ignores the stomatal and cuticular components.

$$v_{ex} = \frac{1}{R_a + R_b + R_{inc} + R_{soil}} \quad (4)$$

The aerodynamic (R_a) and quasi-laminar (R_b) resistances reflect the macro- and molecular-scale turbulence, respectively, between the soil and measurement height of $NH_{3(g)}$. The in-canopy (R_{inc}) and soil (R_{soil}) resistances account for processes within the canopy and at the soil interface that hinder the exchange of gases. According to the theory outlined in Hicks et al. (1987), R_a and R_b can be calculated as such:

$$R_a = \frac{\ln(z_{ref}) - \ln(z_0)}{\kappa \cdot u_*}, \quad (5)$$

$$R_b = \frac{2}{\kappa \cdot u_*} \cdot \left(\frac{Sc}{Pr}\right)^{2/3}, \quad (6)$$

where z_{ref} is the height of the NH_3 measurement (2.7 m), z_0 the roughness length, equal to 0.05 m for uncut grass (Seinfeld and Pandis, 2006), and the von Karman constant $\kappa = 0.4$. The Schmidt number ($Sc = 0.58$) and Prandtl number ($Pr = 0.72$) are taken from Hicks et al. (1987) and account for the diffusivity of NH_3 and heat transfer, respectively. The friction velocity, u_*, can be calculated by

$$u_* = \sqrt[4]{\overline{u'w'}^2 + \overline{v'w'}^2}, \quad (7)$$

where u' and v' are the deviations from the streamline corrected half-hour mean of the horizontal component of wind velocity and w' is the vertical component (Wilczak et al., 2001).

Parameterizations for R_{inc} and R_{soil} vary and are empirically determined through measurements of net vertical flux above a given bulk surface. The former is found to be dependent on the canopy height, season, and land use, whereas the latter is primarily dictated by the Henry's law constant and reactivity of the pollutant. For the present study, values of $R_{inc} = 100\,s\,m^{-1}$ and $R_{soil} = 60\,s\,m^{-1}$ are employed based on the work by Wesely (1989). These values correspond to resistances for a range land in midsummer with lush vegetation and a soil pH of 6.

It should be reiterated that using Eqs. (3) to (7) to estimate soil–atmosphere NH_3 fluxes neglects any vegetative effects (e.g. recapture of NH_3, stomatal emission) and that this serves only as an approximation of NH_3 fluxes between the soil and the atmosphere.

2.3 Soil measurements

Measurements of soil [NH_4^+], pH, and temperature were necessary for calculating the χ. Soil cores were collected in triplicate on 6 days during the campaign, all within 30 feet of the atmospheric measurement inlet. The sampling methodology outlined below is based on work done by Li et al. (2012) and van Miegroet (1995). Samples were collected six times throughout the campaign on the days listed in Table 1. Sites 1, 2, and 3 correspond to small ($\sim 1\,m^2$) areas 10 m west, directly below, and 10 m east of the sonic anemometer, respectively. The soil was sampled more frequently towards the end of the campaign since meteorology (i.e. precipitation, air temperature) was more variable and was expected to perturb the Γ_{soil} to a greater extent than in August when meteorological conditions were more consistent. Specifically, the ranges in air and soil temperature were larger in September than in August. After removing grass and any residual litter (of which there was very little), a PVC tube (5.1 cm inner diameter) was inserted into the ground to a depth of 10 cm and a soil core was removed by pulling out the tube with a soil core intact. Each core was thoroughly mixed and an ~ 8 g subsample was immediately placed into a pre-weighed extract solution (50 mL of 0.25 % KCl w/w) and transported on ice back to the lab for analysis. After shaking for 30 min, extracts were gravity filtered (ashless filter #40, Whatman Ltd., Maidstone, UK) then sent through a 0.2 µm PES membrane syringe filter (Pall Ion Chromatography Acrodisc®, VWR International, Mississauga, ON). Ammonium, nitrate, and nitrite were then quantified using two ion chromatograph (IC) ICS-2000 systems (Dionex Inc., Sunnyvale, CA) operated with suppressed conductivity detection and reagent-free eluent (potassium hydroxide for anions, methanesulfonic acid for cations). Gradient elution schemes were optimized so that analyte peaks were baseline resolved. CS12A analytical and CG12A guard columns were used for the cation IC, and AS19 analytical and AG19 guard columns for the anion IC. In both cases, 25 µL loops were used. ICs were calibrated by injection of commercially available (Dionex Corp., Sunnyvale, CA) mixed standards of seven anions (F^-, Cl^-, NO_2^-, Br^-, NO_3^-, SO_4^{2-}, PO_4^{3-}) and six cations (Li^+, Na^+, NH_4^+, K^+, Mg^{2+}, Ca^{2+}). Serial dilutions of the standards in matrix-matched 0.25 % KCl allowed for a five-point calibration which yielded reasonable calibration curves (slope of $R^2 > 0.99$) for all analytes. Extraction with a 0.25 % KCl solution proved sufficient to desorb all accessible ions in the soil matrix, yet dilute enough to allow for quantification of NH_4^+ and NO_3^- in every sample. The inherent assumption is that the extract solution sufficiently mimics the ability of soil pore water to liberate NH_4^+ ions from the soil matrix to participate in soil–air exchange. An additional extraction into deionized water (DIW) was performed on one set of soil samples. The [NH_4^+] measured in the DIW extract was between 30–45% of that measured with the KCl extraction. Extraction into DIW is an absolute lower bound on soil [NH_4^+] since higher ionic strength solutions will desorb more NH_4^+, and soil pore water has a much higher ionic strength than DIW. Flechard et al. (2013) and Cooter et al. (2010) have suggested fundamental analytical research is required to assess the validity of this assumption, but this is outside the scope of this current study. A field blank was run with every triplicate to account for any contamination (always less than 1 % of the measured soil [NH_4^+]) from sample handling and extraction.

Soil pH was measured by mixing ~ 10 g of soil with an equal mass of deionized water (1:1 soil:DIW slurry). A standard pH electrode (SympHony 14002-782, VWR

Table 1. Soil parameters measured in this study.

Date	Site	$[NH_4^+]$ (mg kg^{-1} wet soil)	pH (1 : 1 slurry soil : deionized water)	Average Γ_{soil} ($\pm 1\sigma$)
13 August	1	1.4	6.9	978 ± 750
	2	1.67	7.3	
	3	0.85	7	
28 August	1	1.43	6.6	290 ± 110
	2	0.31	7	
	3	0.87	6.9	
13 September	1	1.31	5.81	51 ± 20
	2	0.17	6.87	
	3	0.51	6.09	
20 September	1	1.01	5.8	176 ± 140
	2	0.89	6.81	
	3	0.94	6.53	
25 September	1	2.1	6.22	172 ± 43
	2	0.6	6.57	
	3	0.93	6.59	
27 September	1	0.61	6.16	91 ± 40
	2	0.46	6.59	
	3	0.25	6.95	

International, Mississauga, ON) was immediately immersed in the slurry until a stable pH reading was obtained. This was done in triplicate for each soil core, and an average pH for each was calculated. Performing the pH measurements in a saline solution of 0.25 % KCl desorbs more H^+ and was found to lower the pH reading by up to 1 unit relative to extraction into deionized water, which has been reported previously (e.g. Walker et al., 2014). Soil temperature was logged hourly using five in situ sensors (iButtons, Maxim Integrated, San Jose, CA) placed 10 cm deep dispersed across the 30 foot radius of the soil sampling area. Moisture content was determined gravimetrically for a subsample (~ 3 g) of each core by drying in an oven at 105 °C for at least 24 h.

2.4 Atmospheric measurements

Ambient $NH_{3(g)}$ mixing ratios were needed to infer both the direction and magnitude of soil–atmosphere fluxes. Measurements of NH_4^+, SO_4^{2-}, NO_3^- in $PM_{2.5}$ and their precursor gases (SO_2, and HNO_3) were also important to aid in interpretation of air mass trajectory. These water-soluble gases and ions in $PM_{2.5}$ were measured continuously online every hour with the Ambient Ion Monitor Ion Chromatographs (AIM-IC) system (Model 9000D, URG, Chapel Hill, NC). The set-up has been explained in detail elsewhere (Markovic et al., 2012) and is described here only briefly. Ambient air is pulled at 3 L min^{-1} through a $PM_{2.5}$ impactor to remove coarse particles. Gases are stripped from the sample flow by a liquid parallel plate denuder with a 2 mm H_2O_2 solution continuously flowing over the surface. Particles have sufficient inertia to pass through the denuder assembly and enter a supersaturated steam condensation coil where they are grown hygroscopically and collected as an aqueous solution. The aqueous sample then travels through a 22 m sample line to the IC systems where the ~ 5 mL aliquots (collected over an hour) are separately injected and quantified for water soluble ions. The inlet box was mounted on a tower 3 m above the ground.

The AIM-IC was deployed using CS17 and AS19 analytical columns, CG17 and AG19 guard columns, and TCC-ULP1 and TAC-ULP1 concentrator columns. Suppressed conductivity detection and reagent-free gradient elution were used. Five-point calibrations were performed at the beginning, middle, and end of the campaign. Standard solutions of known concentration were made by serial dilution of commercially available standards of mixed anions and cations discussed in the previous section.

Backgrounds were acquired by overflowing the inlet with high-purity zero air for 24 h and averaging the peak area signal acquired. This average peak area was subtracted from the peak areas obtained while sampling ambient air. Detection limits were determined by taking 3 times the standard deviation of the peak area during the final 20 h of the zero air experiment and converting it to either a mixing ratio or mass loading using the calibration curves and assuming a flow of 3 L min^{-1}, pressure of 760 mm Hg and temperature of 298 K.

Atmospheric species of primary interest for this study are NH_4^+, SO_4^{2-}, NO_3^- in $PM_{2.5}$ and their precursor gases (NH_3,

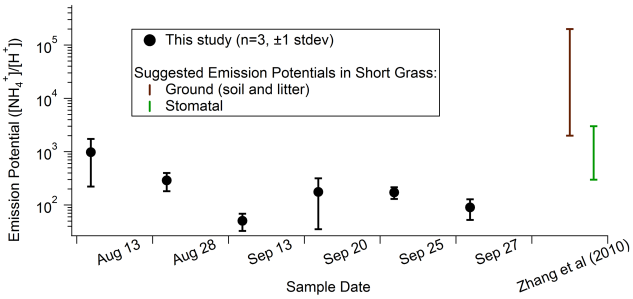

Figure 2. Soil emission potentials (Γ_{soil}) measured throughout this study. Black circles represent the average of three measurements $\pm 1\sigma$. A review by Zhang et al. (2010) suggests Γ ranges for ground (Γ_g) and stomata (Γ_{stom}) for low and high nitrogen input grasslands. These ranges are shown in brown (Γ_g) and green (Γ_{stom}).

SO_2, and HNO_3), for which the limits of detection were 0.2, 0.003, and 0.008 ppb for NH_3, SO_2, and HNO_3, respectively. For NH_4^+, SO_4^{2-}, and NO_3^- in the particle phase the detection limits were 0.025, 0.04, and 0.04 µg m^{-3}, respectively.

Friction velocity (u_*) parameters were calculated from wind velocity measured with a 3-D sonic anemometer (model CSAT3, Campbell Scientific, Logan, UT) operating at 10 Hz. Hourly relative humidity (RH) and air temperature (in °C) at CARE were measured by an Environment Canada weather station located 20 m north of the sonic anemometer. This data was obtained from the Environment Canada website (http://climate.weather.gc.ca/data_index_e.html).

The Hybrid Single-Particle Lagrangian Integrated Trajectory (HYSPLIT) model was used to compute 48 h back-trajectories throughout the campaign in order to assess air parcel history (Draxler and Rolph, 2013). The model was run four times per day with parcels arriving at a height of 100 m above CARE at 02:00, 08:00, 14:00, and 20:00 LT. Resolution of the meteorology model (EDAS) was set to 40 by 40 km.

3 Results and discussion

3.1 Soil emission potential measurements

Figure 2 shows the measured Γ_{soil} for the six soil sampling dates in this study. Soil [NH_4^+] and pH measurements used to determine the Γ_{soil} are shown in Table 1. The variation in Γ_{soil} was up to an order of magnitude on some days (13 August and 20 September) yet was more consistent on others (i.e. 13 and 25 September). Both August dates have the highest Γ_{soil} suggesting there might be some seasonal variability, as has been observed for stomatal emission potentials (Γ_{stom}) (Loubet et al., 2002). However, a similar trend cannot be confirmed for this study due to the relatively short time frame and the inherent heterogeneity of soil. Also shown in Fig. 2 is the range of ground emission potentials (Γ_g) in grasslands suggested by Zhang et al. (2010). Γ_g includes both soil and litter, but during this study there was a negligible amount of litter on the ground; therefore, Γ_g and Γ_{soil} should be analogous. The suggested range in Γ_g (2000 to 200 000) is based on 14 values from six studies, all of which were in fertilized grasslands. Of these studies, only two (David et al., 2009; Mattsson et al., 2009) directly measured Γ_g, whereas the other four either inferred it from measurements of dead or dying leaves (Herrmann et al., 2009; Mattsson and Schjoerring, 2003) or modelled it (Burkhardt et al., 2009; Personne et al., 2009). All the Γ_{soil} values (35 to 1850) measured in this study are below the range from the Zhang et al. (2010) review, likely because the field at CARE is non-fertilized and so has a lower N content. Suggested ranges of Γ_g from Zhang et al. (2010) for various land types were recently incorporated into a regional air quality model (STILT-Chem) by Wen et al. (2013) to allow for bi-directional exchange. The authors found the updated model, using $\Gamma_g = 2000$ over grasslands, overestimates $NH_{3(g)}$ in sites with lower $NH_{3(g)}$ concentrations (i.e. CARE). This could be a consequence of overestimating Γ_g in these regions, as implied by the Γ_{soil} measurements given here.

Massad et al. (2010) carried out a similar review and suggested that Γ_g be parameterized as 500 in non-fertilized, semi-natural environments without vegetation. To our knowledge, the results presented here represent the first values of Γ_{soil} directly measured in a non-fertilized grassland. These measurements underscore the importance of distinguishing between fields that receive fertilization and those that do not. The Γ_g range from Zhang et al. (2010) is not applicable to the field at CARE, whereas the estimation ($\Gamma_g = 500$) from Massad et al. (2010) is more suitable.

It is worth comparing Γ_{soil} to the range of stomatal emission potentials (Γ_{stom}) in grasslands proposed by Zhang et al. (2010) (Fig. 2, green line). Γ_{stom} values (300 to 3000) are based on roughly 50 measurements from over two dozen studies which reflect the narrower range in Γ_{stom} compared to Γ_g. Massad et al. (2010) also parameterized Γ_{stom}, but did so by empirically fitting measurements to total annual N input instead of using a constant value for each land use type. These suggested Γ_{stom} values from each review are on the same order as the Γ_{soil} measured in this study, suggesting that in a non-fertilized field, the soil and vegetation might have a very similar propensity to either emit or uptake NH_3 (i.e. they likely have similar χ).

3.2 Inferred soil compensation point and fluxes

A linear interpolation of Γ_{soil} between the six sampling dates in combination with hourly soil temperature measurements were used to generate a time series of soil compensation point χ_{soil} (black trace in Fig. 3a) according to Eq. (2). The shaded region around χ_{soil} was calculated from a linear interpolation of $\pm 1\sigma$ in Γ_{soil} measurements and therefore reflects the uncertainty in χ_{soil} attributed to variability in soil pH and

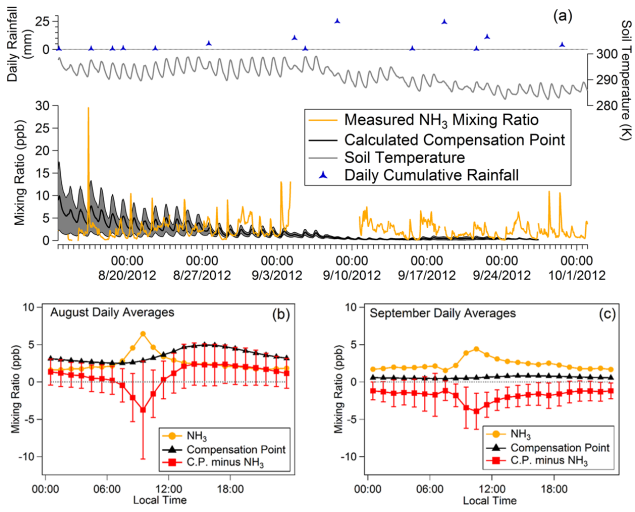

Figure 3. Time series of NH_3 mixing ratio ([NH_3], orange trace), χ_{soil} (black trace), daily cumulative rainfall (blue markers) and soil temperature (T_{soil}, grey trace) throughout the campaign **(a)**. χ_{soil} was calculated using a linear interpolation of Γ_{soil} and hourly soil temperature measurements. The shaded region around χ_{soil} was calculated by linear interpolation of $\pm 1\sigma$ of Γ_{soil} and reflects the uncertainty in χ_{soil} as a result of uncertainty in Γ_{soil} measurements. Panels **(b)** and **(c)** show time of day plots for the average [NH_3], χ_{soil}, and difference between the two (χ_{soil} – [NH_3], red trace) for August and September, respectively. Errors bars in **(b)** and **(c)** represent $\pm 1\sigma$ and are only included for the difference trace for clarity.

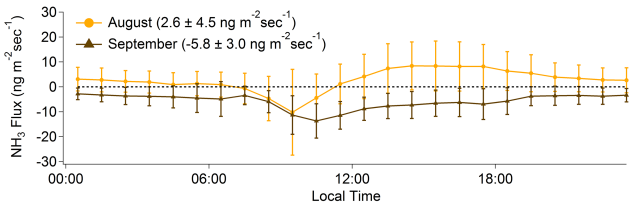

Figure 4. Time-of-day plot showing the average hourly NH_3 flux in August (orange trace) and September (brown trace). A positive flux indicates emission from the soil, whereas a negative flux indicates deposition from the atmosphere.

[NH_4^+]. Hourly gas-phase NH_3 measured by the AIM-IC (orange trace) is also shown. These two traces frequently cross meaning that repeated switching between soil emission and atmospheric deposition is predicted. There is a clear decline in χ_{soil} throughout the campaign that is mostly attributable to a decrease in soil temperature (T_{soil}) as shown by the grey trace at the top of Fig. 3a. Precipitation can also be important factor for NH_3 fluxes – both Cooter et al. (2010) and Walker et al. (2013) observed emission "pulses" of NH_3 over agricultural soils within 24 h after rainfall. Elevated [NH_3] levels are seen on 13 August, 28 August, and 22 September following 0.4 mm, 5.0 mm, and 10.9 mm of rain. Reasons for this could include increased soil NH_4^+ available for exchange, increased diffusion of NH_3 through soil, and/or increased N inputs to the surface as a result of wet deposition.

There is a diurnal trend in χ_{soil} with lower values during the night-time that is a consequence of T_{soil} and has been observed before for stomatal compensation points (Van Hove et al., 2002). It is possible there is a diurnal trend in Γ_{soil} that is not captured by the periodic soil sampling regime. However, this is unlikely since additional measurements from a nearby site found that spatial heterogeneity in soil [NH_4^+] was much larger than the temporal variability in 24 soil grabs taken 6 h apart (soil grabs were in triplicate) over the course of 2 days.

The χ_{soil} diurnal trends are more evident in Fig. 3b and c, which show time-of-day plots for August and September, respectively. During both months, NH_3 peaks between 08:00–10:00 in the morning and is typically at a minimum during the evening where it plateaus at around 2 ppb, which has been observed previously in the region (e.g. Ellis et al., 2011). Mixing ratios were fairly similar in both months, although the morning peak in August was larger than in September. On the other hand, χ_{soil} values were significantly lower in September as a result of lower soil temperatures. Accordingly, the diurnal profiles of the difference between χ_{soil} and [NH_3] (red trace) in Fig. 3b and c are distinct. In August, the difference between χ_{soil} and [NH_3] is positive throughout the majority of the day (excluding 07:00–11:00 in the morning), indicating a net flux from the soil to the atmosphere. On the other hand, in September the difference is negative throughout the entire day, meaning the soil is a continuous sink for atmospheric NH_3. This suggests a clear transition from the soil being a net source to a net sink for NH_3 due to lower soil temperatures. It should be noted that grass senescence had not yet begun and that there was no appreciable accumulation of litter, which has been shown to act as a strong source of NH_3 (e.g. David et al., 2009; Mattsson et al., 2009; Mattsson and Schjoerring, 2003).

In order to determine the magnitude of this exchange, the ν_{ex} was estimated using Eqs. (4) to (7) and the flux was calculated from Eq. (3). The diurnal profile of NH_3 fluxes (in $ng\,m^{-2}\,s^{-1}$) for both months is shown in Fig. 4. Throughout August there is an average net NH_3 emission from the soil of $2.6 \pm 4.5\,ng\,m^{-2}\,s^{-1}$. In September, there was an average net deposition of $5.8 \pm 3.0\,ng\,m^{-2}\,s^{-1}$ from the atmosphere to the surface. Average fluxes measured by Wichink Kruit et al. (2007) were $4\,ng\,m^{-2}\,s^{-1}$ in summer and $-24\,ng\,m^{-2}\,s^{-1}$ in autumn, which are of the same order of the flux values estimated in this study. Wichink Kruit et al. (2007) used their measured fluxes to infer a canopy emission potential (Γ_{canopy}) using data points where cuticular deposition can be neglected (dry conditions) and stomatal exchange is dominant (daytime). Exchange with the soil is ignored in their study due to the low soil pH (about pH = 5); however, this would not be a valid assumption in this study as the soil pH at CARE is about 7, as shown in Table 1. Nonetheless, the inferred Γ_{canopy} was 2200 and is higher than the Γ_{soil} measured in this study. At least to a first

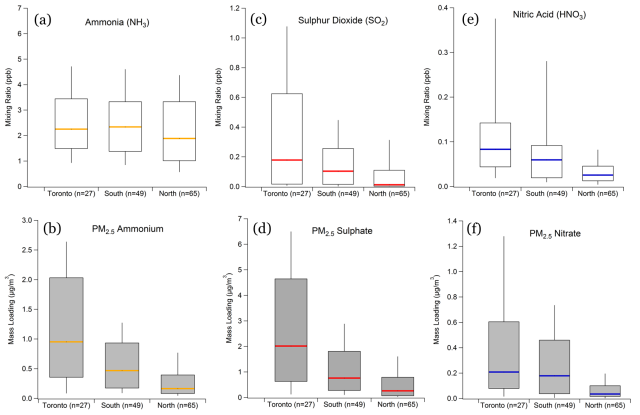

Figure 5. Atmospheric concentrations of **(a)** NH_3, **(b)** particulate NH_4^+, **(c)** SO_2, **(d)** particulate SO_4^{2-}, **(e)** HNO_3, and **(f)** particulate NO_3^- binned by air mass origin calculated from HYSPLIT back-trajectories every 6 h throughout the campaign. The line denotes the median value, the interquartile range is encompassed within the box, and the end of the whiskers are the 10th and 90th percentiles. The number of back-trajectories in each bin is given on the *x* axis in brackets.

approximation, it appears that NH_3 fluxes in both these non-fertilized fields are comparable. The larger deposition in the autumn in Wichink Kruit et al. (2007) is likely attributable to higher NH_3 mixing ratios (~ 9 ppb average versus ~ 2 ppb September average in this study). It is noteworthy that both sites are considered the same land type but likely have very different canopy-level processes driving NH_3 fluxes. Specifically, the soil in Wichink Kruit et al. (2007) had a sufficiently low pH (~ 5) to suppress appreciable soil–atmosphere exchange, which is not the case at CARE. Furthermore, a review by Schlesinger and Hartley (1992) estimate volatilization rates of NH_3 from undisturbed grasslands are between 0.3 and 30 $ng\,m^{-2}\,s^{-1}$, which encompasses the values from this work and that of Wichink Kruit et al. (2007).

It is also important to consider wet deposition when assessing net exchange of NH_3 between the atmosphere and an ecosystem. The Canadian Air and Precipitation Monitoring Network (CAPMoN) collects daily precipitation samples at CARE and reports the results online (http://www.on.ec.gc.ca/capmon/login/login.aspx). The average NH_4^+ wet deposition rates from 2001–2011 for August and September are $12.4 \pm 4.6\,ng\,m^{-2}\,s^{-1}$ and $11.3 \pm 5.4\,ng\,m^{-2}\,s^{-1}$, respectively. In the context of our results (fluxes of $2.6 \pm 4.5\,ng\,m^{-2}\,s^{-1}$ in August and $-5.8 \pm 3.0\,ng\,m^{-2}\,s^{-1}$ in September), the site at CARE has net NH_3 deposition in both months when one considers both wet deposition and bi-directional exchange. In other words, the magnitude of wet deposition fluxes is roughly 2–5 times larger than the magnitude of bi-directional exchange. However, it is important to note that wet deposition occurs in discrete events, whereas dry exchange is continuous.

3.3 Evidence for bi-directional exchange

Since CARE lies on a sharp gradient between high NH_3 emissions to the south and low emissions to north (Fig. 1), one might expect air masses from the north to be lower in NH_3 relative to air masses from the south. Similarly, the greater level of anthropogenic activity south of CARE suggests an enrichment of anthropogenic pollutants (i.e. SO_2, SO_4^{2-}, HNO_3 and NO_3^-) in air masses from the south. In order to interrogate this hypothesis, 2-day back-trajectories were calculated using the Hybrid Single Particle Lagrangian Integrated Trajectory (HYSPLIT) model for every 6 h throughout the study. Each 6-hour time stamp was then classified as having had the air mass pass through Toronto (a box defined from 43.5–44.0° N by 79.0–80.0° N), or having originated from the north (spent more than half its time above 44.23° N) or the south (spent more than half its time below 44.23° N and not passing through Toronto). Results from this analysis are shown in Fig. 5 and yield a distinct directional bias for all species except NH_3; air masses passing through Toronto are clearly enhanced in SO_2, HNO_3, NH_4^+, SO_4^{2-}, and NO_3^- but not NH_3. A lack of directional bias for NH_3 could be explained by proximity to a large NH_3 source, but as seen in Fig. 1, there is a sharp regional (tens of kilometres) gradient in the emissions inventory suggesting that no such local source exists. A more likely explanation is that bi-directional exchange of NH_3 between the surface and atmosphere modulates near-surface NH_3 mixing ratios sufficiently to eliminate any directional bias that would result from traditional emission sources.

Considering the relatively low Γ_{soil} and small magnitude of soil fluxes, it is reasonable to ask whether such an exchange could have a noticeable effect on observed NH_3 mixing ratios. First, a simple calculation was performed to see if the soil reservoir contained enough NH_4^+ to sustain fluxes during the month of August. To do this, the following assumptions were made: NH_3 exchange occurs in the top 10 cm of soil, the soil is equilibrating a 1000 m atmospheric boundary layer, and soil density is 1.5 $g\,cm^{-3}$. Figure 6 shows that even during peak soil emission in the afternoon, less than 1 % of the soil NH_4^+ pool is required to equilibrate the entire boundary layer. Furthermore, much of this lost soil NH_4^+ would be regained during the inferred morning deposition event. Considering that the turnover time for most soil NH_4^+ pools is of the order of a day (Booth et al., 2005), it is safe to assume that there is sufficient NH_4^+ in non-fertilized grasslands to maintain fluxes to the atmosphere.

Second, this exchange could only sufficiently impact NH_3 mixing ratios if it occurs quickly enough. To test this, fast (0.005 $m\,s^{-1}$, at 14:00) and slow (0.003 $m\,s^{-1}$, at 01:00) average exchange velocities from August were used to calculate the time it would take the system (soil and atmosphere) to arrive halfway to equilibrium with an atmospheric height of 1000 m, as well as with the height at which AIM-IC measurements were made (3 m). For 1000 m, the timescale

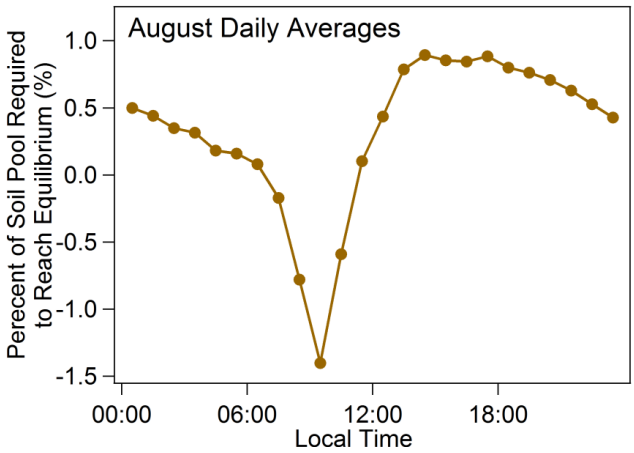

Figure 6. Estimated percent of the soil NH_4^+ pool required to equilibrate with the boundary layer (assumed to be 1000 m) using the average fluxes during August. The top 10 cm of the soil exchanges, and the soil density is $10\,g\,cm^{-1}$ (i.e. there are no units for "soil exchanges"). Positive values indicate fluxes are from the soil to the atmosphere (i.e. the soil is losing NH_4^+).

is calculated to be between 40 and 62 h for the fast and slow ν_{ex}, respectively. However, for a height of 3 m, only 7 and 11 min are required to get halfway to equilibrium. Although this calculation neglects vertical mixing beyond 3 m (which will occur), these short timescales suggest soil–atmosphere exchange is an important component of observed negative $[NH_{3(g)}]$ gradients with height. In other words, soil–atmosphere exchange over non-fertilized grasslands has the ability to strongly influence near-surface NH_3 despite the low Γ_{soil} (relative to fertilized fields) whereas the impact on NH_3 levels throughout the boundary layer is dampened due to slower exchange.

3.4 Morning increase of NH_3

A morning increase in $NH_{3(g)}$ between 08:00–10:00 is clearly evident in Fig. 3b and c and has been observed elsewhere (e.g. Bash et al., 2010; Ellis et al., 2011; Flechard et al., 2013; Nowak et al., 2006; Wichink Kruit et al., 2007). The factors contributing to this phenomenon at CARE are not entirely clear but may include one or more of the following: dew evaporation, volatilization of particulate NH_4NO_3, emission from plants/soil, and/or mixing down of NH_3 rich air entrained above the nocturnal boundary layer. Wichink Kruit et al. (2007) observed a similarly timed increase that coincided with a decrease in leaf wetness. Furthermore, Flechard et al. (1999) and Bussink et al. (1996) found that water layers sorbed on leaves can store significant quantities of NH_3 even at an RH below 100 %. Although no leaf wetness sensor was employed during this study, we use night-time RH as a surrogate for dew and fog formation. Figure 7 shows the difference between the morning NH_x ($\equiv NH_{3(g)} + NH^+_{4(particle)}$) and the average overnight NH_x concentration.

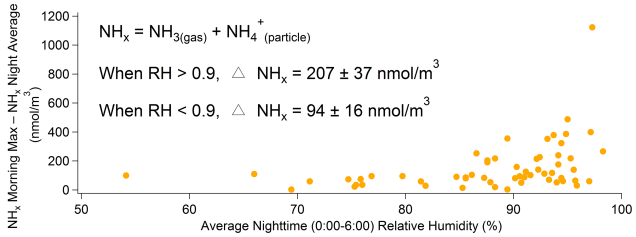

Figure 7. The magnitude of the morning NH_x ($\equiv NH_{3(g)} + NH^+_{4(particle)}$) peak subtracted from the night-time (00:00–6:00) NH_x average versus the average night-time relative humidity. The latter was used as a surrogate for dew formation. The average Δ NH_x ($\pm 1\sigma_{mean}$) both above and below RH = 0.9 are shown inset in the figure.

NH_x was chosen to eliminate any bias caused by volatilization of $NH_4NO_{3(p)}$ to $NH_{3(g)}$ and $HNO_{3(g)}$ as temperatures rise. Mornings following a night during which RH was above 0.9 had an average Δ NH_x of $207 \pm 37\,nmol\,m^{-3}$, whereas increases during mornings following drier nights (RH < 0.9) were about half that, with an average $94 \pm 16\,nmol\,m^{-3}$. Although the RH benchmark of 0.9 only serves as a surrogate for dew formation, this finding does suggest that pools of surface water (i.e. dew or fog), which form on nights that have a high RH, can act as significant NH_x reservoirs that release NH_3 upon evaporation in the mid-morning. This is corroborated by measurements from Burkhardt et al. (2009), who reported an approximate water film thickness of 0.1 mm during dew events and an average dew $[NH_4^+]$ of $3.5\,mg\,kg^{-1}$ in a grassland canopy. If all of the NH_4^+ were to be released as $NH_{3(g)}$ upon dew evaporation, this reservoir would release about $20\,\mu mol\,m^{-2}$ of $NH_{3(g)}$ into the atmosphere, which corresponds to an increase of $20\,nmol\,m^{-3}$ throughout a 1000 m boundary layer, equivalent to an increase in mixing ratio of 0.5 ppb. Such a release could have a significant impact on near surface $NH_{3(g)}$ measurements and manifest itself as a large morning increase of $NH_{3(g)}$. The role of dew and fog as a night-time reservoir definitely merits further investigation and could be an important process within this bi-directional framework. Since NH_x morning increases plateau at $\sim 100\,nmol\,m^{-3}$ at an RH below 0.85, there are likely other contributing factor(s) that lead to this morning enhancement of NH_3. Bash et al. (2010) observed a similar morning rise over a fertilized corn field and attributed it to plant and/or soil processes. However, CARE contains significantly less vegetation and is non-fertilized. Walker et al. (2013) suggested surface–air NH_3 exchange is impacted by ions that can accumulate in dew as well as the pH of the dew. In addition, Fig. 4 reveals there are predicted deposition fluxes to the soil during the morning. It is highly unlikely that a substantial rise in Γ_{soil} could occur over the span of a few hours. Stomatal emission cannot be conclusively ruled out as a significant contribution. However, if this were an important factor, one would expect sunrise (when stomata open) and

the spike to coincide, but given that sunrise at CARE was between 06:00 and 07:15 throughout the campaign, stomatal emission is not likely the driving factor behind this trend at CARE. It is also possible this morning increase is linked to the break-up of the nocturnal boundary layer, as observed by Walker et al. (2006), who measured surface NH_3 fluxes over a fertilized soya bean field. Observations from this study rule out soil emissions and suggest that dew/fog evaporation plays a key role in enhancing morning NH_3 mixing ratios.

4 Conclusions

Measurements of Γ_{soil} and T_{soil} in a non-fertilized grassland were used to construct a time series of χ_{soil} over a 50-day period. Γ_{soil} ranged from 35 to 1850 with an average value of 290, which is well below the $2000 < \Gamma_g < 200\,000$ suggestion by Zhang et al. (2010) for grasslands. Zhang et al. (2010) recommended this range based on field studies exclusively in fertilized grasslands, which is likely the reason Γ_g values in this study are lower. Indeed the distinction between fertilization and non-fertilization is critical in accurately assessing bi-directional exchange. Our findings are more in line with the parameterizations of Massad et al. (2010), who suggested a Γ_g of 500 for semi-natural, non-fertilized areas without vegetation. Seasonal and diurnal trends in χ_{soil} were observed with lower values at night and in September due to decreases in T_{soil}.

Fluxes of NH_3 between the soil and atmosphere were estimated using $[NH_{3(g)}]$ measurements and a simple resistance scheme that neglects the influence of vegetation. August fluxes were primarily upwards, except between 07:00–11:00, and resulted in an average emission of $2.6 \pm 4.5\,\mathrm{ng\,m^{-2}\,s^{-1}}$ from the soil. September was characterized by exclusive deposition from the atmosphere at a rate of $5.8 \pm 3.0\mathrm{ng\,m^{-2}\,s^{-1}}$. These values are fairly similar to fluxes measured by Wichink Kruit et al. (2007), who reported fluxes of 4 and $-24\,\mathrm{ng\,m^{-2}\,s^{-1}}$ in the summer and autumn, respectively.

HYSPLIT analysis revealed that air masses passing through Toronto were enriched in atmospheric pollutants except NH_3. Since CARE lies on a sharp gradient of high emissions to the south and low emission to the north, this lack of directional bias implies that bi-directional exchange efficiently modulates NH_3 mixing ratios. Back-of-the-envelope calculations confirm that: (1) the reservoir of NH_4^+ in soil of non-fertilized grasslands is large enough to sustain fluxes to the atmosphere and (2) fluxes are rapid enough to impact surface concentrations on a relevant timescale.

Figure 7 suggests that dew and fog evaporation can enhance the frequently observed morning increase in NH_3. It is unlikely that soil emissions contribute to this increase as deposition to the soil is predicted during the morning.

More research is needed to explore seasonal and annual trends in Γ_{soil}, $\Gamma_{stomata}$, and χ_{canopy} across all land types, particularly those lacking in measurements. Since regional-scale models require these parameters as direct inputs, there is great utility in taking a "bottom-up" approach (i.e. measuring Γ instead of inferring it from flux data). Even though non-fertilized fields have lower nitrogen content, evidence provided here suggests surface–atmosphere exchange can still affect near-surface concentrations and that this process should be considered when measuring ambient NH_3 over non-fertilized surfaces. The role of fog and dew as a night-time reservoir for water-soluble gases also requires further attention as it may greatly enhance morning NH_3 concentrations and is currently not incorporated in models.

Acknowledgements. The AIM-IC was available through support to J. G. Murphy from the Canada Foundation for Innovation and the Ontario Research Fund. G. R. Wentworth and P. K. Gregoire acknowledge funding from the NSERC Integrating Atmospheric Chemistry and Physics from Earth to Space (IACPES) program. The authors are grateful to Environment Canada and the staff at CARE, as well as Greg Evans and Cheol-Heon Jeong for providing a mobile lab to house the instrumentation during the campaign.

Edited by: S. M. Noe

References

Bash, J. O., Walker, J. T., Katul, G. G., Jones, M. R., Nemitz, E., and Robarge, W. P.: Estimation of in-canopy ammonia sources and sinks in a fertilized Zea mays field., Environ. Sci. Technol., 44, 1683–1689, 2010.

Bash, J. O., Cooter, E. J., Dennis, R. L., Walker, J. T., and Pleim, J. E.: Evaluation of a regional air-quality model with bidirectional NH_3 exchange coupled to an agroecosystem model, Biogeosciences, 10, 1635–1645, doi:10.5194/bg-10-1635-2013, 2013.

Bates, R. G. and Pinching, G. D.: Dissociation constant of aqueous ammonia at 0–50 °C from E.m.f. studies of the ammonium salt of a weak acid, Am. Chem. J., 72, 1393–1396, 1950.

Booth, M. S., Stark, J. M., and Rastetter, E.: Controls on nitrogen cycling in terrestrial ecosystems: a synthetic analysis of literature data, Ecol. Monogr., 75, 139–157, 2005.

Burkhardt, J., Flechard, C. R., Gresens, F., Mattsson, M., Jongejan, P. A. C., Erisman, J. W., Weidinger, T., Meszaros, R., Nemitz, E., and Sutton, M. A.: Modelling the dynamic chemical interactions of atmospheric ammonia with leaf surface wetness in a managed grassland canopy, Biogeosciences, 6, 67–84, doi:10.5194/bg-6-67-2009, 2009.

Bussink, D. W., Harper, L. A., and Corré, W. J.: Ammonia transport in a temperate grassland: II. Diurnal fluctuations in response to weather and management conditions, Agron. J., 86, 621–626, 1996.

Cooter, E. J., Bash, J. O., Walker, J. T., Jones, M. R., and Robarge, W.: Estimation of NH_3 bi-directional flux from managed agricultural soils, Atmos. Environ., 44, 2107–2115, 2010.

Cooter, E. J., Bash, J. O., Benson, V., and Ran, L.: Linking agricultural crop management and air quality models for regional

to national-scale nitrogen assessments, Biogeosciences, 9, 4023–4035, doi:10.5194/bg-9-4023-2012, 2012.

Dasgupta, P. K. and Dong, S.: Solubility of ammonia in liquid water and generation of trace levels of standard gaseous ammonia, Atmos. Environ., 20, 565–570, 1986.

David, M., Loubet, B., Cellier, P., Mattsson, M., Schjoerring, J. K., Nemitz, E., Roche, R., Riedo, M., and Sutton, M. A.: Ammonia sources and sinks in an intensively managed grassland canopy, Biogeosciences, 6, 1903–1915, doi:10.5194/bg-6-1903-2009, 2009.

Draxler, R. R. and Rolph, G. D.: HYSPLIT (Hybrid Single-Particle Lagrangian Integrated Trajectory) Model access via NOAA ARL READY Website, available at: http://www.arl.noaa.gov/HYSPLIT.php (last access: 20 February 2014), NOAA Air Resources Laboratory, College Park, MD, 2014.

Ellis, R. A., Murphy, J. G., Markovic, M. Z., VandenBoer, T. C., Makar, P. A., Brook, J., and Mihele, C.: The influence of gas-particle partitioning and surface-atmosphere exchange on ammonia during BAQS-Met, Atmos. Chem. Phys., 11, 133–145, doi:10.5194/acp-11-133-2011, 2011.

Farquhar, G. D., Firth, P. M., Wetselaar, R., and Weir, B.: On the gaseous exchange of ammonia between leaves and the environment: determination of the ammonia compensation point, Plant Physiol., 66, 710–714, 1980.

Flechard, C. R., Sutton, M. A., and Cape, J. N.: A dynamic chemical model of bi-directional ammonia exchange between semi-natural vegetation and the atmosphere, Q. J. Roy. Meteor. Soc., 125, 2611–2641, 1999.

Flechard, C. R., Massad, R.-S., Loubet, B., Personne, E., Simpson, D., Bash, J. O., Cooter, E. J., Nemitz, E., and Sutton, M. A.: Advances in understanding, models and parameterizations of biosphere–atmosphere ammonia exchange, Biogeosciences, 10, 5183–5225, doi:10.5194/bg-10-5183-2013, 2013.

Herrmann, B., Mattsson, M., Jones, S. K., Cellier, P., Milford, C., Sutton, M. A., Schjoerring, J. K., and Neftel, A.: Vertical structure and diurnal variability of ammonia exchange potential within an intensively managed grass canopy, Biogeosciences, 6, 15–23, doi:10.5194/bg-6-15-2009, 2009.

Hicks, B. B., Baldocchi, D. D., Meyers, T. P., Hosker, R. P., and Matt, D. R.: A preliminary multiple resistance routine for deriving dry deposition velocities from measured quantities, Water Air Soil Pollut., 36, 311–330, 1987.

Krupa, S.: Effects of atmospheric ammonia (NH_3) on terrestrial vegetation: a review, Environ. Pollut., 124, 179–221, 2003.

Li, K., Zhao, Y., Yuan, X., Zhao, H., Wang, Z., Li, S., and Malhi, S. S.: Comparison of factors affecting soil nitrate, nitrogen, and ammonium nitrogen extraction, Commun. Soil Sci. Plant Anal., 43, 571–588, 2012.

Loubet, B., Milford, C., Hill, P. W., Tang, Y. S., Cellier, P., and Sutton, M. A.: Seasonal variability of apoplastic NH_4^+ and pH in an intensively managed grassland, Plant Soil, 238, 97–110, 2002.

Markovic, M. Z., VandenBoer, T. C., and Murphy, J. G.: Characterization and optimization of an online system for the simultaneous measurement of atmospheric water-soluble constituents in the gas and particle phases, J. Environ. Monit., 14, 1872–1884, 2012.

Massad, R.-S., Nemitz, E., and Sutton, M. A.: Review and parameterisation of bi-directional ammonia exchange between vegetation and the atmosphere, Atmos. Chem. Phys., 10, 10359–10386, doi:10.5194/acp-10-10359-2010, 2010.

Mattsson, M. and Schjoerring, J. K.: Senescence-induced changes in apoplastic and bulk tissue ammonia concentrations of ryegrass leaves, New Phytol., 160, 489–499, 2003.

Mattsson, M., Herrmann, B., David, M., Loubet, B., Riedo, M., Theobald, M. R., Sutton, M. A., Bruhn, D., Neftel, A., and Schjoerring, J. K.: Temporal variability in bioassays of the stomatal ammonia compensation point in relation to plant and soil nitrogen parameters in intensively managed grassland, Biogeosciences, 6, 171–179, doi:10.5194/bg-6-171-2009, 2009.

Milford, C., Theobald, M. R., Nemitz, E., and Sutton, M. A.: Dynamics of ammonia exchange in response to cutting and fertilising in an intensively-managed grassland, Water Air Soil Poll., 1, 167–176, 2001.

Mosquera, J., Hensen, A., Van den Bulk, W. C. M., Vermeulen, A. T., and Erisman, J. W.: Long term NH_3 flux measurements above grasslands in the Netherlands, Water Air Soil Poll., 1, 203–212, 2001.

National Pollutant Release Inventory: 2008 Ammonia Emissions for Canada: http://www.ec.gc.ca/inrp-npri/donnees-data/ap/index.cfm?lang=En (last access: 30 January 2014), 2011.

Nemitz, E., Sutton, M. A., Schjoerring, J. K., Husted, S., and Paul Wyers, G.: Resistance modelling of ammonia exchange over oilseed rape, Agr. Forest Meteorol., 105, 405–425, 2000.

Nemitz, E., Milford, C., and Sutton, M. A.: A two-layer canopy compensation point model for describing bi-directional biosphere-atmosphere exchange of ammonia, Q. J. Roy. Meteor. Soc., 127, 815–833, 2001.

Nemitz, E., Sutton, M. A., Wyers, G. P., and Jongejan, P. A. C.: Gas-particle interactions above a Dutch heathland: I. Surface exchange fluxes of NH_3, SO_2, HNO_3 and HCl, Atmos. Chem. Phys., 4, 989–1005, doi:10.5194/acp-4-989-2004, 2004.

Nowak, J. B., Huey, L. G., Russell, A. G., Tian, D., Neuman, J. A., Orsini, D., Sjostedt, S. J., Sullivan, A. P., Tanner, D. J., Weber, R. J., Nenes, A., Edgerton, E., and Fehsenfeld, F. C.: Analysis of urban gas phase ammonia measurements from the 2002 Atlanta Aerosol Nucleation and Real-Time Characterization Experiment (ANARChE), J. Geophys. Res., 111, D17308, doi:10.1029/2006JD007113, 2006.

Personne, E., Loubet, B., Herrmann, B., Mattsson, M., Schjoerring, J. K., Nemitz, E., Sutton, M. A., and Cellier, P.: SURFATM-NH3: a model combining the surface energy balance and bi-directional exchanges of ammonia applied at the field scale, Biogeosciences, 6, 1371–1388, doi:10.5194/bg-6-1371-2009, 2009.

Pleim, J. E., Bash, J. O., Walker, J. T., and Cooter, E. J.: Development and evaluation of an ammonia bidirectional flux parameterization for air quality models, J. Geophys. Res. Atmos., 118, 3794–3806, 2013.

Pope, C. A., Burnett, R. T., Thun, M. J., Calle, E. E., Krewski, D., and Thurston, G. D.: Lung cancer, cardiopulmonary mortality, and long-term exposure to fine particulate air pollution, J. Am. Med. Assoc., 287, 1132–1141, 2002.

Reis, S., Pinder, R. W., Zhang, M., Lijie, G., and Sutton, M. A.: Reactive nitrogen in atmospheric emission inventories, Atmos. Chem. Phys., 9, 7657–7677, doi:10.5194/acp-9-7657-2009, 2009.

Rupakheti, M., Leaitch, W. R., Lohmann, U., Hayden, K., Brickell, P., Lu, G., Li, S.-M., Toom-Sauntry, D., Bottenheim, J. W.,

Brook, J. R., Vet, R., Jayne, J. T., and Worsnop, D. R.: An intensive study of the size and composition of submicron atmospheric aerosols at a rural site in Ontario, Canada, Aerosol Sci. Tech., 39, 722–736, 2005.

Schlesinger, W. H. and Hartley, A. E.: A global budget for atmospheric NH_3, Biogeochemistry, 15, 191–211, 1992.

Seinfeld, J. H. and Pandis, S. N.: Atmospheric Chemistry and Physics: From Air Pollution to Climate Change, 2nd edn., John Wiley & Sons, Toronto, 2006.

Spindler, G., Teichmann, U., and Sutton, M. A.: Ammonia dry deposition over grassland – micrometeorlogical flux-gradient measurements and bidirectional flux calculations using an inferential model, Q. J. Roy. Meteor. Soc., 127, 795–814, 2001.

Su, H., Cheng, Y., Oswald, R., Behrendt, T., Trebs, I., Meixner, F. X., Andreae, M. O., Cheng, P., Zhang, Y., and Pöschl, U.: Soil nitrite as a source of atmospheric HONO and OH radicals., Science, 333, 1616–1618, 2011.

Sutton, M. A., Fowler, D., Moncrieff, J. B., and Storeton-West, R. L.: The exchange of atmospheric ammonia with vegetated surfaces, II: Fertilized vegetation, Q. J. Roy. Meteor. Soc., 119, 1047–1070, 1993.

Sutton, M. A., Schjorring, J. K., Wyers, G. P., Duyzer, J. H., Ineson, P., and Powlson, D. S.: Plant-atmosphere exchange of ammonia, Philos. Trans. Phys. Sci. Eng., 351, 261–278, 1995.

Sutton, M. A., Milford, C., Dragosits, U., Place, C. J., Singles, R. J., Smith, R. I., Pitcairn, C. E. R., Fowler, D., Hill, J., ApSimon, H. M., Ross, C., Hill, R., Jarvis, S. C., Pain, B. F., Phillipd, V. C., Harrison, R., Moss, D., Webb, J., Espenhahn, S. E., Lee, D. S., Hornung, M., Ullyett, J., Bull, K. R., Emmett, B. A., Lowe, J., and Wyers, G. P.: Dispersion, deposition and impacts of atmospheric ammonia: quantifying local budgets and spatial variability, Environ. Pollut., 102, 349–361, 1998.

Sutton, M. A., Milford, C., Nemitz, E., Theobald, M. R., Hill, P. W., Fowler, D., Mattsson, M. E., Nielsen, K. H., Husted, S., Erisman, J. W., Otjes, R., Hensen, A., Mosquera, J., Cellier, P., Loubet, B., David, M., Genermont, S., Neftel, A., Blatter, A., Herrmann, B., Jones, S. K., Horvath, L., Führer, E. C., Mantzanas, K., Koukoura, Z., Williams, P., Flynn, M., and Riedo, M.: Biosphere-atmosphere interactions of ammonia with grasslands: experimental strategy and results from a new European initiative, Plant Soil, 228, 131–145, 2001.

Sutton, M. A., Nemitz, E., Milford, C., Campbell, C., Erisman, J. W., Hensen, A., Cellier, P., David, M., Loubet, B., Personne, E., Schjoerring, J. K., Mattsson, M., Dorsey, J. R., Gallagher, M. W., Horvath, L., Weidinger, T., Meszaros, R., Dämmgen, U., Neftel, A., Herrmann, B., Lehman, B. E., Flechard, C., and Burkhardt, J.: Dynamics of ammonia exchange with cut grassland: synthesis of results and conclusions of the GRAMINAE Integrated Experiment, Biogeosciences, 6, 2907–2934, doi:10.5194/bg-6-2907-2009, 2009.

Van Hove, L. W.., Heeres, P., and Bossen, M..: The annual variation in stomatal ammonia compensation point of rye grass (*Lolium perenne* L.) leaves in an intensively managed grassland, Atmos. Environ., 36, 2965–2977, 2002.

Van Miegroet, H.: Inorganic nitrogen determined by laboratory and field extractions of two forest soils, Soil Sci. Soc. Am. J., 59, 549–553, 1995.

Walker, J. T., Robarge, W. P., Wu, Y., and Meyers, T. P.: Measurement of bi-directional ammonia fluxes over soybean using the modified Bowen-ratio technique, Agr. Forest Meteorol., 138, 54–68, 2006.

Walker, J. T., Jones, M. R., Bash, J. O., Myles, L., Meyers, T., Schwede, D., Herrick, J., Nemitz, E., and Robarge, W.: Processes of ammonia air–surface exchange in a fertilized *Zea mays* canopy, Biogeosciences, 10, 981–998, doi:10.5194/bg-10-981-2013, 2013.

Walker, J. T., Robarge, W. P., and Austin, R.: Modeling of ammonia dry deposition to a pocosin landscape downwind of a large poultry facility, Agric. Ecosyst. Environ., 185, 161–175, 2014.

Wen, D., Zhang, L., Lin, J. C., Vet, R., and Moran, M. D.: An evaluation of ambient ammonia concentrations over southern Ontario simulated with different dry deposition schemes within STILT-Chem v0.8, Geosci. Model Dev. Discuss., 6, 6075–6115, doi:10.5194/gmdd-6-6075-2013, 2013.

Wesely, M. L.: Parameterization of surface resistances to gaseous dry deposition in regional-scale numerical models, Atmos. Environ., 23, 1293–1304, 1989.

Wichink Kruit, R. J., van Pul, W. A. J., Otjes, R. P., Hofschreuder, P., Jacobs, A. F. G., and Holtslag, A. A. M.: Ammonia fluxes and derived canopy compensation points over non-fertilized agricultural grassland in the Netherlands using the new gradient ammonia – high accuracy – monitor (GRAHAM), Atmos. Environ., 41, 1275–1287, 2007.

Wichink Kruit, R. J., van Pul, W. A. J., Sauter, F. J., van den Broek, M., Nemitz, E., Sutton, M. A., Krol, M., and Holtslag, A. A. M.: Modeling the surface–atmosphere exchange of ammonia, Atmos. Environ., 44, 945–957, 2010.

Wichink Kruit, R. J., Schaap, M., Sauter, F. J., van Zanten, M. C., and van Pul, W. A. J.: Modeling the distribution of ammonia across Europe including bi-directional surface–atmosphere exchange, Biogeosciences, 9, 5261–5277, doi:10.5194/bg-9-5261-2012, 2012.

Wilczak, J. M., Oncley, S. P., and Stage, S. A.: Sonic anemometer tilt correction algorithms, Bound.-Lay. Meteorol., 99, 127–150, 2001.

Zhang, L., Wright, L. P., and Asman, W. A. H.: Bi-directional air-surface exchange of atmospheric ammonia: a review of measurements and a development of a big-leaf model for applications in regional-scale air-quality models, J. Geophys. Res., 115, D20310, doi:10.1029/2009JD013589, 2010.